

# Numerical investigation of cyclic performance of frames equipped with tube-in-tube buckling restrained braces

Shahrokh Maalek<sup>1</sup>, Hamid Heidary-Torkamani<sup>\*2</sup>,  
Moharram Dolatshahi Pirooz<sup>1</sup> and Seyed Taghi Omid Naeeni<sup>1</sup>

<sup>1</sup> School of Civil Engineering, College of Engineering, University of Tehran, Iran

<sup>2</sup> School of Civil Engineering, College of Engineering, University of Tehran, Tehran, Iran

(Received August 31, 2017, Revised April 10, 2018, Accepted January 26, 2019)

**Abstract.** In this research, the behavior of tube-in-tube BRBs (TiTBRBs) has been investigated. In a typical TiTBRB, the yielding core tube is located inside the outer restraining one to dissipate energy through extensive plastic deformation, while the outer restraining tube remains essentially elastic. With the aid of FE analyses, the monotonic and cyclic behavior of the proposed TiTBRBs have been studied as individual brace elements. Subsequently, a detailed finite element model of a representative single span-single story frame equipped with such a TiTBRB has been constructed and both monotonic and cyclic behavior of the proposed TiTBRBs have been explored under the application of the AISC loading protocol at the braced frame level. With the aid of backbone curves derived from the FE analyses, a simplified frame model has been developed and verified through comparison with the results of the detailed FE model. It has been shown that, the simplified model is capable of predicting closely the cyclic behavior of the TiTBRB frame and hence can be used for design purposes. Considering type of connection detail used in a frame, the TiTBRB member which behave satisfactorily at the brace element level under cyclic loading conditions, may suffer global buckling due to the flexural demand exerted from the frame to the brace member at its ends. The proposed TiTBRB suit tubular members of offshore structures and the application of such TiTBRB in a typical offshore platform has been introduced and studied in a single frame level using detailed FE model.

**Keywords:** tube-in-tube buckling restrained brace; buckling restrained braced frame; offshore platforms; cyclic loading; FE analysis

## 1. Introduction

In recent years, buckling-restrained braced frames (BRBFs), which refer to concentrically-braced frames that include buckling-restrained braces (BRBs), are increasingly used as the primary lateral force resisting system in seismic prone areas. The first reported test on buckling-restrained braces has been conducted by Kimura *et al.* (Takeda *et al.* 1976). Since then, a number of experimental and analytical studies have been carried out for the development of conventional concrete filled BRBs (e.g., Fahnestock *et al.* 2003, Lopez *et al.* 2004, Sabelli *et al.* 2003, Watanabe *et al.* 1988) and to introduced a unified design procedure for the seismic design of steel buckling-restrained braced frames (BRBFs) (e.g., (Fahnestock *et al.* 2007a, b, Kersting *et al.* 2015). Hence, special design recommendations have been incorporated into Seismic Provisions for Structural Steel Buildings (AISC 341-10 2010).

A conventional configuration of BRBs consists of a steel core encased in a mortar/concrete filled steel tube, which restrains the core plate against buckling in compression and results in a stable hysteretic curve accompanied by enhanced ductility. Considerable attentions have also been

paid to all-steel BRBs with core plates (e.g., Della Corte *et al.* 2014, Korzekwa and Tremblay 2009, Piedrafita *et al.* 2015, Tremblay *et al.* 2006). In the latter type of BRBs, similar to concrete-filled BRBs, the core members are made up of steel plates restrained by steel elements. In all-steel BRBs, the concrete works are excluded and the core plate is supported by steel restrainers and connectors without any mortar/concrete and unbonding materials.

The present work is concerned with a new type of all-steel BRB system in which steel core and the external restraining member are made up of Circular Hollow Sections (CHSs) located concentrically without any infilled concrete or mortar; instead, intermediate rings are used to make it possible for the external tube to act as the restrainer to prevent buckling of the interior core tube. Thus there is no need for the application of unbonding materials around the steel core. In this manner, the fabrication steps associated with applying the unbonding materials, pouring and curing the concrete or mortar are excluded that considerably reduces manufacturing costs and time. In addition, the lighter weight of such all-steel BRBs-compared with the ones with infilled concrete-are associated with ease and speed of fabrication, transportation, erection, inspection, disassembly and replacement. This type of BRB system was introduced by Ghasemi (2006), Maalek and Ghasemi (2010), Omidi (2014) and Fotoohabadi (2015). Here, this type of BRB

\*Corresponding author, Ph.D. Student,  
E-mail: [Hamid\\_heidary@ut.ac.ir](mailto:Hamid_heidary@ut.ac.ir)

member is referred to as the Tube-in-Tube BRB (TiTBRB) system.

Despite potential advantages of Tube-in-Tube BRB (TiTBRB) systems, research works on such members have been very limited and hence further studies are needed before a comprehensive design guidance can be presented. In a TiTBRB member, a rather identical behavior is expected to be exhibited by the inner core under both tension and compression when its buckling is prevented by means of the outer restating tube. Thus a stable hysteretic loop is expected to be observed under the application of a cyclic loading.

The idea of the use of tube-in-tube members with intermediate rings as buckling restrained braces was developed as a result of observations made by Maalek (1999) during experimental works carried out on double Circular Hollow Sections (CHS). As described in details, in the works reported by Maalek (1999) and Maalek and Ghasemi (2010), during the construction of an aircraft hangar, tests had been performed on double CHSs to explore the potentiality of the use of a tube-in-tube section instead of a larger size single section which was not manufactured at the time by Iranian tube manufacturers. Hence, two series of tube-in-tube members had been constructed and tested: the members in which there was no intermediate connection between tubes along their lengths, as suggested by the project contractor, and the specimens in which intermediate rings had been employed to provide transverse load transmission between the inner tubes and the external ones. The rings had been employed at intervals along the inner tube length with a proper thickness, welded by spot welding to the inner tube, in order to provide just a minimum clearance to let the passage of the outer tube. In this manner, it was expected that with the initiation of buckling in either of the tubes followed by a small lateral deflection, the two tubes would come into contact and act together. The results showed that the ultimate load of the tube-in-tube member acting together through the intermediate ring was 1.75 times the maximum load of the member without such a filler ring. The above observations led to the development of the idea of the use of tube-in-tube elements, as BRB members. In the case of tube-in-tube BRB which is considered in the present study, the role of the outer tube is to prevent buckling of the inner one which is intended to act as the structural core of a BRB member during cyclic loading.

It should be emphasized that the experiments on the tube in tube columns with and without filler rings have been noted here in order to demonstrate the manner in which the idea of the Tube in Tube BRB members, discussed here, originated and developed. However, in the case of BRBs, the load-carrying behavior is quite different from double tube column. In the case of BRBs, the load-carrying behavior is quite different from double tube columns.

Ghasemi (2006) and Maalek and Ghasemi (2010) introduced BRB members composed of double circular hollow sections, one located inside the other. Through a series of detailed finite element analyses calibrated by laboratory test results, it was demonstrated that the introduced double-tube/tube-in-tube member was capable

of achieving the intended tasks as a buckling restrained bracing member. The cyclic and monotonic behavior of the introduced Tube-in-Tube BRB members was further investigated by Omidi (2014). Two specimens with different lengths (i.e., 3 m and 6 m) were considered and investigated numerically through a series of finite element analyses. Based on the results, it was shown that the proposed Tube-in-Tube BRB had a desirable hysteretic performance under cyclic loading. Fotoohabadi (2015) extended the previous investigations towards the application of Tube-in-Tube BRBs in actual steel frames to compare the seismic performance of special concentrically braced frames (SCBFs) and frames equipped with the TiTBRBs. A full-scale 5-story building was designed based on the AISC specifications (AISC 360-10 2010) and seismic provisions (AISC 341-10 2010) considering both the SCBF system as well as the proposed BRBF. Three scaled ground motion records were used to conduct the nonlinear dynamic analysis to compare the seismic response of the building structure under consideration. The static pushover analyses were also performed for further comparison of the SCBF and BRBF performances under monotonically displacement control loading. On the basis of results, the seismic performance of the prototype framed structures equipped with TiTBRB was found to be superior to the SCBF system.

The present authors, during this current study, learned about the works of Yin *et al.* (2011), Yin and Wang (2010) and Yin and Bu (2016) published recently, well after the works reported in (Ghasemi 2006) and Maalek and Ghasemi (2010). In this series of research, the performance of double steel-tube BRBs has been studied through numerical simulation and small-scale experimental tests. It has been reported that the double-tube BRB with contact rings prevented the buckling of the core member to enable yielding under both compression and tension, (Yin and Wang 2010). In another research, Dongbin *et al.* (2016) have proposed a BRB system using three concentric circular steel tubes in which the slotted middle tube has been considered to act as the yielding core and the outer and inner tubes restrain the out-of-plane deformation of the core tube. In the work, no mention has been made about the actual gaps necessary for the passage of inner tubes through the outer ones in the test specimens, depending on available tube sizes and permissible tolerance. A comprehensive parametric investigation has been performed by (Heidary-Torkamani and Maalek 2017) involving the influential parameters affecting the behaviour and modes of failure of the TiTBRBs during cyclic loading through detailed finite element analysis procedures accounting for material and geometric nonlinearities as well as the effects of gaps and contacts.

Previous researches have demonstrated that BRBs are capable of withstanding large cumulative ductility demands (Fahnestock *et al.* 2007a). Although the ductility capacity of individual BRB members has been clearly established but, less attention has been paid to the ability of BRBs to develop their full ductility capacity when situated in actual frames. In other words, as shown by previous researchers (e.g., (Fahnestock *et al.* 2003, 2007a, b), in addition to BRB individual behavior, the behavior of such BRB members

when installed in a frame (i.e., the behavior of the complete buckling restrained braced frames (BRBFs)) should also be investigated meticulously. In this regard, in the present study, once the individual TiTBRB is proposed and analyzed through detailed finite element modeling and analysis, the behavior of such TiTBRB members has also been explored within a one span-one story frame level composed of such TiTBRBs.

### 1.1 Research plan

The step by step framework outlined in the current study is as follows;

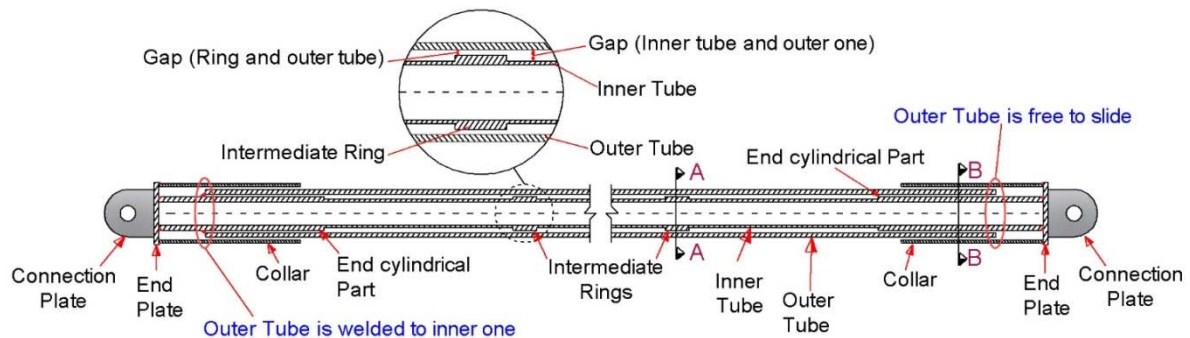
- The fundamental concepts of the behavior of the Tube-in-Tube BRBs (TiTBRBs) have been explained as an efficient kind of all-steel BRBs.
- A 3.5×5 single span-single story steel frame has been designed in order to investigate the behavior of the proposed TiTBRB at the frame level.
- Two TiTBRB members with different values of restraining ratios representing the external tube stiffness have been designed in such a way that they can be situated in the aforementioned frame.
- The designed individual TiTBRBs have been simulated numerically by using ABAQUS finite element package. Their monotonic and cyclic behaviors have been investigated according to the AISC seismic provisions.
- Based on the results of numerical analyses, the backbone curve, as well as the corresponding equivalent viscose damping ratio have been

determined.

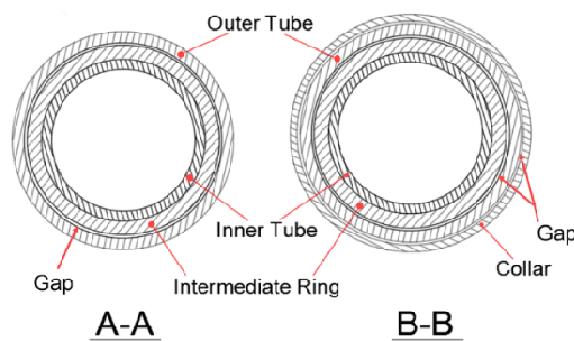
- The analyzed TiTBRBs have then been situated in the steel frame with pin connections. The detailed FE models of the frames equipped with the TiTBRBs has then been constructed with the use of solid elements. Subsequently, the numerical models have been analyzed under monotonic and hysteretic loading conditions to the AISC loading protocol.
- The frame has also been modeled using nonlinear beam (frame) elements. Multilinear backbone curve extracted for the TiTBRB member has been assigned to the brace element in order to simulate the TiTBRB behavior. The results obtained on the basis of the detailed finite element modeling has been compared with those obtained by means of the simplified frame/beam model.

## 2. Proposing tube-in-tube BRBs

Based on the intended function, a typical tube-in-tube buckling restrained brace (TiTBRB) is composed of four components; namely: inner core, restraining tube, intermediate rings and end collars. The inner tube is intended to act as the structural core to resist axial loads in such a way that the energy can be appropriately dissipated by its yielding under reversible cyclic loading. On the other hand, the outer tube is supposed to act as the lateral restraint for the inner one without interfering in the axial load carrying of the inner tube; that is, using a gap separating the two tubes, the inner tube should be free to slide inside the



(a) Longitudinal section profile of a typical TiTBRB



(b) Cross-section profile of a typical TiTBRB

Fig. 1 A typical tube-in-tube BRB

outer one. Hence, axial loads are resisted by the inner core tube and the outer tube may only interfere in the axial force carrying through friction at the contact points after the core deforms laterally.

Here, the contact rings are responsible for transverse load transmission between the inner core tube and the external restraining one. In other words, in the initiation of buckling of the inner tube under compressive loading, slight lateral deflection shall lead to the contact between the inner and the outer tubes at points where intermediate rings have been provided. The main purpose in using collar tubes at the ends of a TiTBRB is to prevent the possible local buckling of the exposed part of the core tube under load reversal resulting in high levels of plastic strains at both ends. In the proposed TiTBRB members, the inner core tube has been assumed to be welded to the end plates using full penetration welds. The collar tubes are also assumed to be welded to end plates. The intermediate rings are supposed to be spot welded to the inner tube at proper intervals. A typical TiTBRB with its components is demonstrated in Fig. 1.

### 3. Numerical study of the behavior of the individual TiTBRB member

#### 3.1 Finite element model of the TiTBRB member

In order to identify the cyclic behavior of an individual TiTBRB member to be used at the frame level, two TiTBRB members have been considered and investigated numerically. In both TiTBRB models considered here, the inner core tubes are composed of S235 steel with the identical cross-sectional area to have an equal load-carrying capacity. The outer restraining tube is composed of S355 steel. Introducing the restraining ratio as (1, although the cross-sectional area of the core member in both models is the same, the outer tube cross section (diameter and thickness) has been altered that affects the restraining ratio of the TiTBRB members. All other design related parameters such as the number of the intermediate rings and the amount of gap have been kept unchanged. In addition, a friction coefficient of 0.1 and the initial imperfection value of 6 mm has been adopted for both models. The initial imperfection is considered as the initial lateral deflection of commercially available tubes.

It should be noted that in Eq. (1), the  $P_e(e)$  is the Euler load of the external tube considered as a hinged compressive member and  $P_y(i)$  is the squash load of the inner core tube. The geometric properties of TiTBRB models are presented in Table 1. In addition, the value of restraining ratios is also presented in the table for both models.

$$\Psi = \frac{P_e(e)}{P_y(i)} \quad (1)$$

In order to attain a reasonable understanding of the behavior of the proposed TiTBRB member, numerical simulations have been employed here using ABAQUS software. This software has been recently used for the simulation of other types of buckling restrained braces by a number of researchers e.g., Chou and Chen (2010), Hoveidae *et al.* (2015), Sabelli *et al.* (2003), showing the capability of the 3D finite element modeling of their BRB models, in producing results that are in good agreement with their laboratory test data.

The wall thicknesses of both the inner core tube and the external tube are considerably smaller compared to the other dimensions. Thus, both tubes can be simulated using shell elements in an effort to lessen the computational expense. However, in this study, all parts with circular sections (the core tube, the restraining tube, and the end collars) have been modeled using 3D solid elements in order to capture the following effects.

3D solid elements can be used in the form of linear (C3D8) or quadratic (C3D20) formulation. The use of linear isoparametric continuum elements (C3D8), exhibits some artificial flexural rigidities due to the composed disproportionately large shear-related strain energy. The analyses performed in the present study, introduce a bending-dominated problem (i.e., buckling) which significantly upsurges the unreal flexural rigidity of the model resulting from the shear-locking effect. The reduced-integration linear solid elements (C3D8R) with hourglass control, could alleviate shear-locking effects. However, to capture the TiTBRB bending response more accurately, reduced-integration 20-node hex-quadratic continuum elements, designated as C3D20R in ABAQUS analysis and theory manual (2007), with a minimum of two elements along the wall thickness of each part of the model has been used.

When global buckling occurs, the 3D solid element with a sufficient number of elements through the thickness demonstrates a better representation of stresses across the wall thickness. In addition, using solid elements facilitates characterizing the interaction surface between the core and

Table 1 Geometric properties of TiTBRBs considered in this study

BRB members	Inner Core Tube			Outer Tube			Intermediate Rings			Cylindrical End Part			$G_1^*$	$G_2^{**}$	$\psi$
	OD <sub>i</sub>	t <sub>i</sub>	L <sub>i</sub>	OD <sub>e</sub>	t <sub>e</sub>	L <sub>e</sub>	OD <sub>r</sub>	t <sub>r</sub>	L <sub>r</sub>	OD <sub>c</sub>	t <sub>c</sub>	L <sub>c</sub>			
	(mm)	(mm)	(mm)	(mm)	(mm)	(mm)	(mm)	(mm)	(mm)	(mm)	(mm)	(mm)			
Model 1	114	6.8	4800	154	8	4500	134	10	50	134	10	350	12	2	1.5
Model 2	114	6.8	4800	158	10	4500	134	10	50	134	10	350	12	2	2

\*  $G_1$  is the gap between the outer face of the inner core tube and the inner face of the external tube

\*\*  $G_2$  is the gap between the outer face of the intermediate rings and the inner face of the external tube

Table 2 Material properties of steel alloys used in the current study

	$\sigma_0$ / Equivalent stress	C	$\gamma$	Q-infinity	B	Ref.
	MPa	MPa		MPa		
S235	255.9	26.9	0.0	227.8	5.8	(Jia and Kuwamura 2014)
		1617.2	10.7			
S355	350.0	8000.0	75.0	110.0	4.0	(Mazzolani <i>et al.</i> 2009)
		26.9	0.0			

the restraining tube, and between the external tube and the collars around its ends.

In this study two steel alloys, referred to as S235 and S355, have been used for the core and the external tube respectively. A constitutive nonlinear isotropic/kinematic cyclic hardening model provided by ABAQUS has been implemented in the numerical simulation. The efficiency and accuracy of this combined model have been confirmed in previous studies (Chou and Chen 2010, Dongbin *et al.* 2016, Hoveidae *et al.* 2015, Jiang *et al.* 2015, Sabelli *et al.* 2003, Tremblay *et al.* 2006). The Young's modulus and Poisson's ratio of steel have been considered as 210 GPa and 0.3, respectively. The necessary parameters involving nonlinear materials models, have been acquired from the literature and are presented in Table 2. The definition of the parameters can be found ABAQUS analysis and theory manual (SIMULIA 2007).

According to the ABAQUS user manual, the parameters listed in Table 2 can be described as follows;

In the case of kinematic hardening, " $\sigma_0$ " is the yield stress at zero plastic strain, "C" is the kinematic hardening modulus and " $\gamma$ " indicates the rate at which hardening modulus decreases with plastic strain. While, in the case of isotropic hardening parameter, "Equivalent stress" is the size of the elastic range at zero plastic strain, "Q-infinity" is the maximum change in the size of the yield surface and "b" shows the rate at which  $\sigma_0$  changes with plastic strain (SIMULIA 2007).

Proper modeling of contact interaction between the core tube and the restraining member is a milestone in numerical simulation of a typical TiTBRB. Here, the contact pairs have been established between the inner face of the outer tube and the outer face of the inner core tube, the outer face of contact rings and the inner face of the outer tube as well between the inner face of collar tubes and the outer face of the outer restraining tube. The normal behavior of interaction was modeled using a hard contact behavior, allowing for separation of the interface in tension with no penetration in compression. Applying penalty algorithm provided in ABAQUS, the friction forces between contact pairs are involved in the numerical simulation to provide a greasy interface between the surfaces.

In order to apply axial loading protocol conveniently, a perforated connection plate crossed with a circular end plate is attached at both ends of the core member (see Fig. 2). In the TiTBRB members, end collars and the steel core have

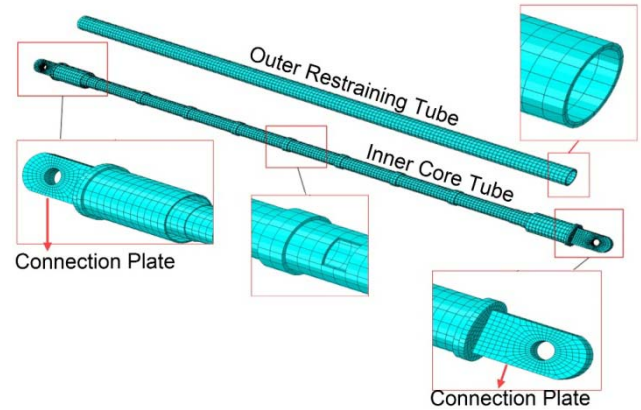


Fig. 2 The finite element model of the TiTBRBs under consideration

been assumed to be welded to the end plates. Accordingly, tie constraints have been considered between the collars and the end plates as well between the core tube and the end plates at both ends. The simple hinged (pinned) connection has been assumed at the center of holes produced at both ends. The connection and end plates are designed to be stiffer than other parts to experience insignificant levels of plastic deformations during loading. This justifies their modeling as linear elastic materials. The finite element model of the TiTBRB and the associated generated mesh is shown in Fig. 2.

### 3.2 Loading protocol

In order to investigate the cyclic performance of TiTBRBs, the displacement loading protocol proposed by

Table 3 Loading protocol used as cyclic loading for individual TiTBRBs

Protocol	No. of cycles	Axial displacement		Inelastic disp.	
		$\Delta_{bm}$	$\Delta_y$	Per cycle	Cumulative
AISC	2	$0.17\Delta_{bm}$	$1.0\Delta_y$	0.0	0.0
	2	$0.50\Delta_{bm}$	$2.9\Delta_y$	15.6	15.6
	2	$1.00\Delta_{bm}$	$5.9\Delta_y$	39.3	54.9
	2	$1.50\Delta_{bm}$	$8.8\Delta_y$	62.9	117.8
	2	$2.00\Delta_{bm}$	$11.8\Delta_y$	86.5	204.3

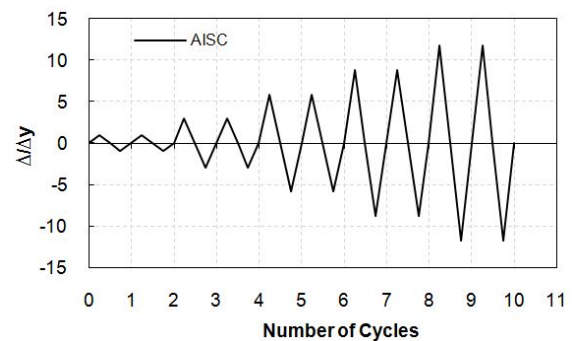


Fig. 3 Displacement protocol used for cyclic loading

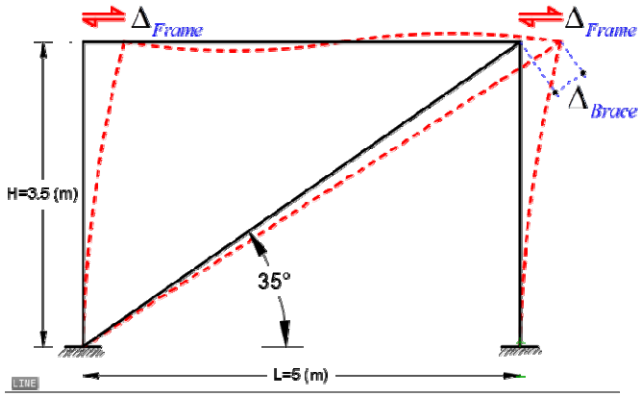


Fig. 4 Frame used for loading protocol determination

the AISC 341-10 (2010) (has been used (see Fig. 3 and Table 3). The term  $\Delta_y$  stands for the displacement that corresponds to the yielding of the inner core tube, and  $\Delta_{bm}$  is the axial deformation of the brace corresponding to the design story drift.

According to the AISC provision, the  $\Delta_{bm}$  was determined based on the story drift of 0.01 as shown in Fig. 4. The calculated value for  $\Delta_{bm}$  was to reach the cumulative inelastic displacement (CID) of 200. In this study, the selected value for  $\Delta_{bm}$  has been 29 (mm) which allows the BRB specimen to reach a CID of 204.

### 3.3 Analysis of individual TiTBRB members under monotonic and cyclic loading

In this section, the individual TiTBRBs has been analyzed under monotonic as well as cyclic loading conditions using the aforementioned loading protocol. The results of the monotonic analysis for the core tube with and without a restraining tube is presented in Fig. 5. It can be seen that under monotonic loading, the results for both of the specimens TiTBRB-1 and TiTBRB-2 lie on each other.

At the element, it can be observed from Figs. 6(a) and (b) that the overall cyclic behavior of the two specimens are very close to each other. The core deflection during the cyclic loading has been captured and is displayed in Fig. 7 at certain displacement values.

### 3.4 TiTBRB backbone curve

For a better illustration of practical application, one model (i.e., TiTBRB-2) is considered for post-processing to calculate a strength adjustment factor and a strain hardening adjustment factor. In addition, the backbone curve is extracted carefully for the model under study. Moreover, equivalent viscous damping is determined as explained in the following subsections. It should be noted that, as it was shown in Fig. 6, the hysteresis load-displacement curve of both TiTBRBs (i.e., TiTBRBs with restraining ratios of 1.5 and 2) is approximately the same resulting in identical

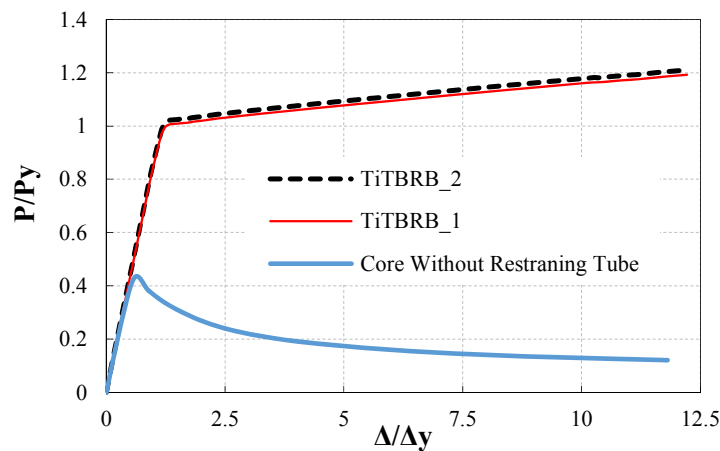
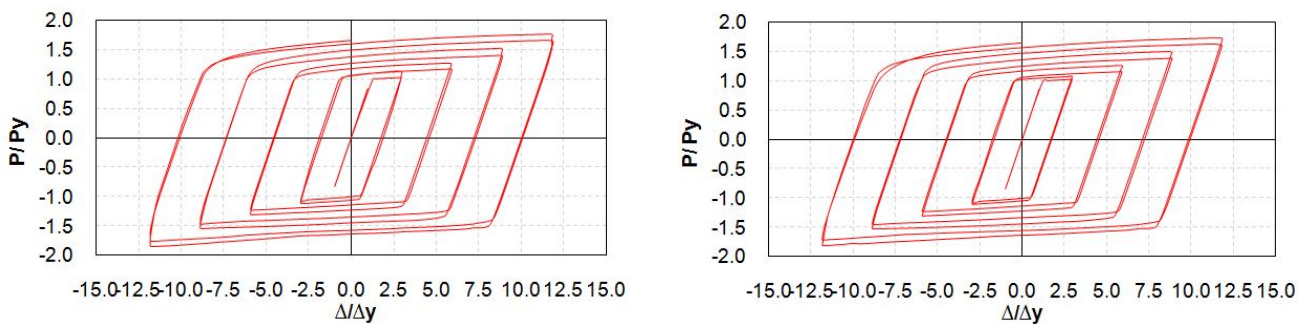


Fig. 5 Monotonic behavior of the TiTBRB under compressive axial load



(a) TiTBRB -1 with a restraining ratio of 1.5

(b) TiTBRB-2 with a restraining ratio of 2

Fig. 6 Cyclic behavior of the TiTBRBs under consideration

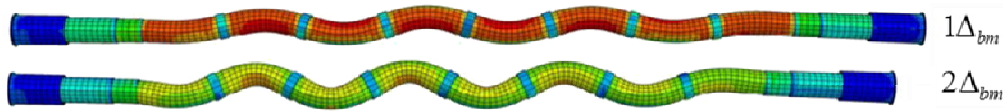


Fig. 7 The deformed shape of the core tube during cyclic compressive loading at axial displacements of  $1\Delta_{bm}$  and  $2\Delta_{bm}$

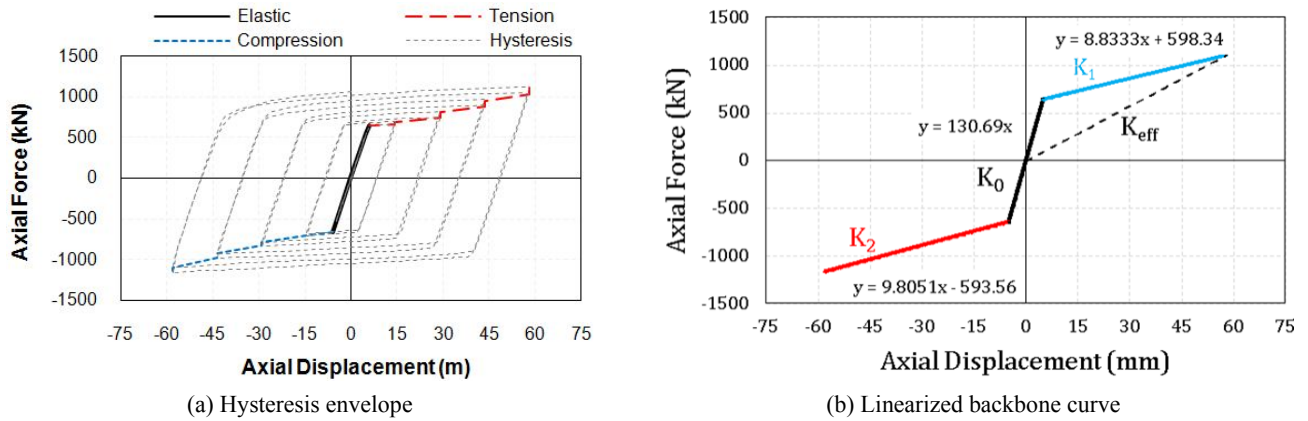


Fig. 8 Backbone curve for TiTBR-2

backbone curve. Hence, the backbone curve is presented here only for TiTBRB-2 with a restraining ratio of 2. It can be seen later in this work that the TiTBRB-1 with the restraining ratio of 1.5 buckles at the final stage of loading due to the exerted flexural moments when the frame deformation becomes large.

In a well-designed BRB specimen, preventing buckling leads to ductile behavior and a rather identical strength in tension and compression, illustrated by the envelope of the hysteresis curves, also referred to as a backbone curve. Backbone curve is an imperative basis of the practical design of a structure intended to be equipped with BRBs. Applying this curve allows designers to extrapolate the constructive cyclic behavior of the steel material to an individual BRB element level. Consequently, the BRB behavior can be extrapolated to overall structure level and thus a structure can be designed using BRBs to dissipate energy.

The backbone curve is obtained for the model under study in the form of both exact hysteresis envelope and linearized one, as shown in Fig. 8. The stiffness values (i.e.  $K_0$ ,  $K_1$ ,  $K_2$ , and  $K_{eff}$ ) are also computed and presented in Fig. 8.

According to the AISC 341-10, the tension-compression asymmetry factor ( $\beta$ ), and tension strain hardening adjustment factor ( $\omega$ ) can respectively be calculated from Eqs. (2) and (3) as follows

$$\beta = \frac{C_{max}}{T_{max}} \quad (2)$$

$$\omega = \frac{T_{max}}{P_{y,core}} = \frac{T_{max}}{f_{y,core} \times A_{core}} \quad (3)$$

where  $C_{max}$  and  $T_{max}$  are the ultimate forces of the TiTBRB

member in compression and tension respectively. Accordingly,  $f_{y,core}$  and  $A_{core}$  are the core yield stress and the core cross-sectional area, respectively. For the model under study, the values of  $\beta$  and  $\omega$  are calculated at each loop of

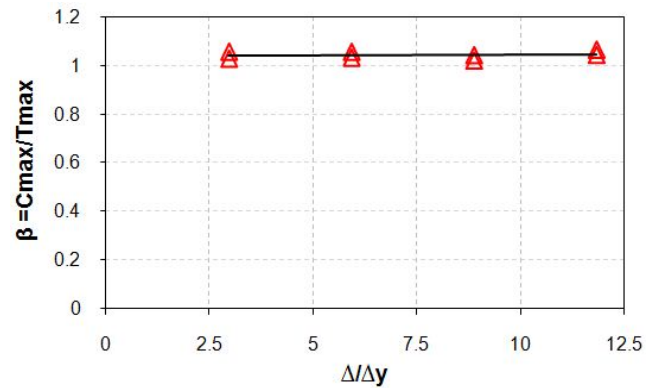


Fig. 9  $\beta$  versus normalized brace deformation

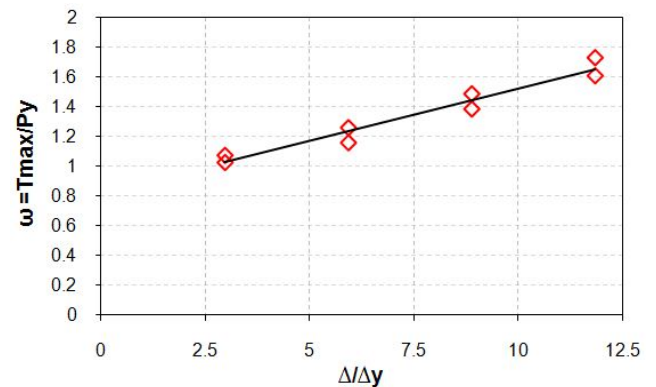


Fig. 10  $\omega$  versus normalized brace deformation

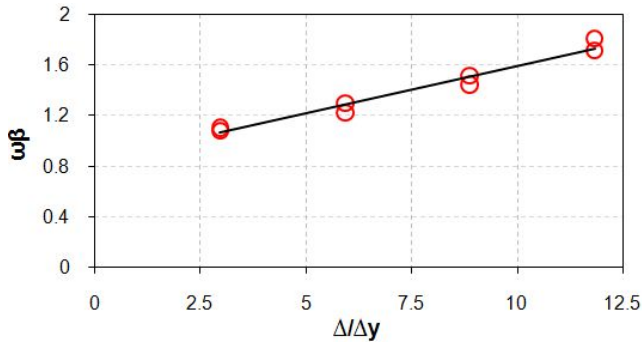


Fig. 11  $\omega\beta$  versus normalized brace deformation

the hysteresis curve and are displayed in Figs. 9 and 10, respectively. The product  $\omega\beta$  versus brace axial displacements is also presented in Fig. 11. The AISC seismic provisions mandate that the compression strength adjustment factor,  $\beta$ , be less than 1.3.

### 3.5 Equivalent ratio of viscous damping

As noted earlier, nowadays different types of BRBs are utilized as the robust lateral force resisting components both in the seismic retrofit of the existing structure and new construction projects. Another application may comprise employing BRBs as supplemental hysteretic metal energy dissipaters in a structural system, which was the primary motivation behind the introduction of the BRBs. Thus, it is of a particular interest to offer a damping index for a BRB specimen by which a quantity can be assigned to the BRB member through simulation and calculation.

In this regard, according to the equation proposed by Clough and Penzien (Clough and Penzien 1993) the equivalent viscous damping,  $\xi_{eq}$ , can be calculated for the TiTBRB member based on the amount of energy dissipated in each hysteretic loop as defined in Eq. (4).

$$\xi_{eq} = \frac{E_h}{4\pi E_e} \quad (4)$$

For a given displacement (i.e., given  $\Delta_{max}$  and  $\Delta_{min}$ ),  $E_h$  is the energy dissipated in a hysteresis cycle, and  $E_e$  is the

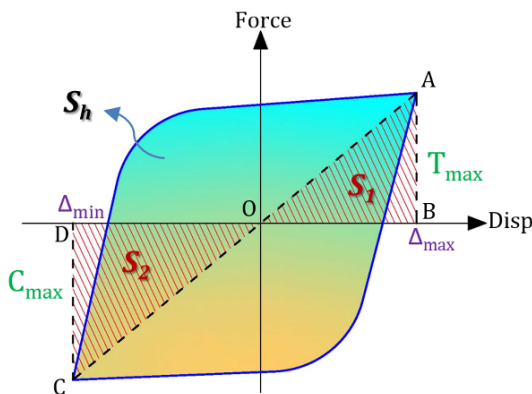


Fig. 12 Illustration of the equivalent ratio of viscous damping

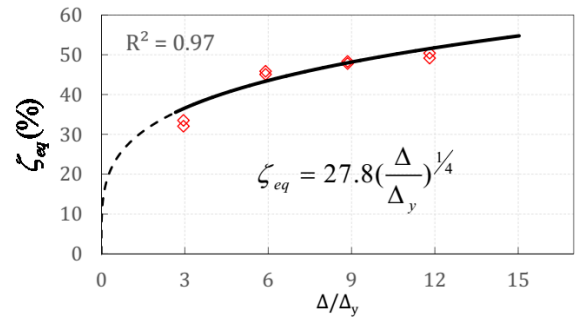


Fig. 13 A sample correlation of equivalent viscose damping for the TiTBRB under study

stored strain energy. According to Fig. 12,  $\xi_{eq}$  can be computed based on areas defined in the figure by applying Eq. (5).  $E_h$  is the area enclosed by the load-deformation response of the TiTBRB in the cycle and  $E_e$  is equal to the average of  $S_1$  and  $S_2$ .

$$\left. \begin{aligned} E_h &= S_h \\ E_e &= \frac{1}{2}(S_1 + S_2) \end{aligned} \right\} \Rightarrow \xi_{eq} = \frac{S_h}{2\pi(S_1 + S_2)} \quad (5)$$

The equivalent ratio of viscous damping values of the specimen under study has been calculated at each cycle of loading protocol as presented in Fig. 13.

As shown in the figure, the equivalent viscous damping ratio has increased gradually with the increase in the loading amplitude. A non-linear regression can then be fitted utilizing the corresponding data as

$$\xi_{eq} = a \left( \frac{\Delta}{\Delta_y} \right)^{1/4} \quad (6)$$

where “a” is a constant, found from such a regression to be equal to 27.8. The obtained value for the “a” constant is consistent with the representative values for this constant for experimentally tested concrete filled BRBs, as presented in work reported by Merritt *et al.* (2003).

## 4. Numerical investigation of the frame equipped with TiTBRB

Up to this point, it has been demonstrated through numerical analyses that the individual tube-in-tube bracing members can be competently regarded as a buckling restrained brace with a good energy dissipation capacity. According to the AISC seismic provisions, for any type of buckling restrained brace, both at the element level and the frame level, experimental tests should be conducted to verify the brace behavior and to extract design related parameters (such as  $\beta$ ,  $\omega$ ). Hence, in order to investigate the behavior of proposed TiTBRB in the frame level, the TiTBRB is modeled together with the beam and columns of a single bay-single story frame and the behavior of such a bracing member in a frame equipped with such BRB members is investigated. The columns are composed of box girder 25 cm  $\times$  25 cm with 25 mm thickness and the beam

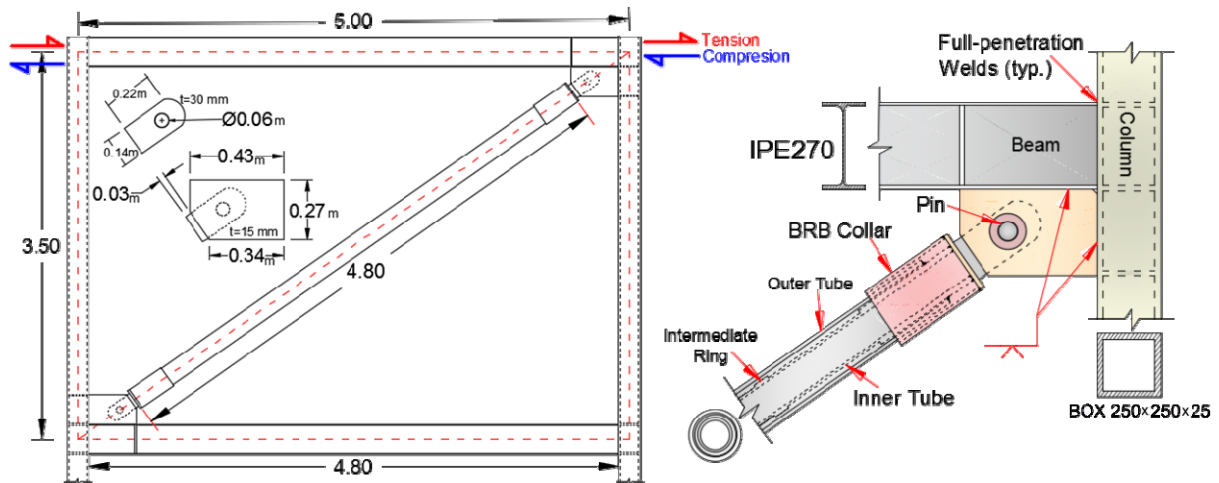


Fig. 14 The single bay-single story frame considered here to be equipped with TiTBRB (TiTBRBF)

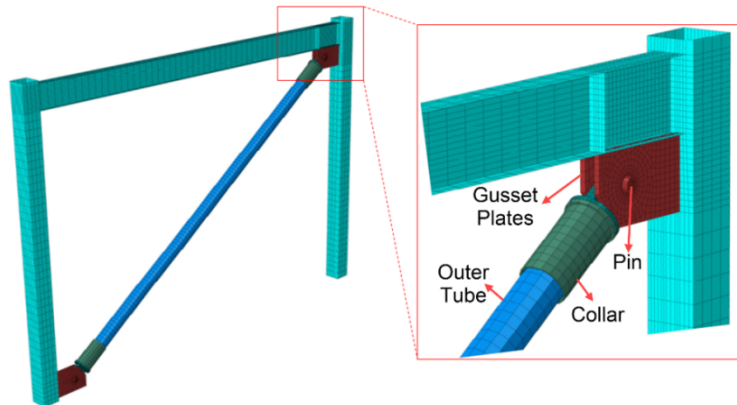


Fig. 15 Finite element model of the single bay-single story frame equipped with TiTBRB using dual gusset plate

is composed of IPE270 as shown in Fig. 14. Two gusset plates have been used on both sides of the bracing member. Using dual gusset plates provides moment resistance at the end of the bracing member to prevent out of plane premature buckling. The TiTBRB member is attached to the gusset plates using connection pins. Here, the frame equipped with TiTBRB system is referred to as the “Tube-in-Tube Buckling Restrained Braced Frame (TiTBRBF)”.

Due to the fact that gusset plates sustain high levels of tensile and compressive stress during cyclic analysis, these plates have been modeled using eight node solid elements (C3D20R) with two elements in the gusset plate wall thickness. The beam and columns have been modeled using 4 nodes reduced integration shell elements (S4R).

In practice, the connection pins are manufactured from ultra-strong steel and loaded in double shear. Accordingly, the pins are noticeably stiffer than the other parts in the TiTBRB member, indicating that the pins can be considered as elastic members in the numerical simulations. Fig. 15 shows the FE model of the TiTBRBF with associated generated mesh.

#### 4.1 Monotonic analysis of the frame equipped with TiTBRB

In this section, a monotonically increasing lateral loading under displacement control has been applied to the frame equipped with TiTBRB (i.e., TiTBRBF). Two TiTBRBs with different values of the restarting ratio (i.e.  $P_e/P_y$  of 2 and 1.5) have been considered in the frame and analyzed monotonically twice in two opposite directions in such a way that the TiTBRB experiences monotonic compressive as well as tensile stresses. The results of these analyses are depicted in Fig. 16. As shown in the figure, in the case of TiTBRB with  $P_e/P_y$  of 1.5, the TiTBRB buckles globally in lateral frame displacement of 64 mm resulting in load deterioration in the load-displacement curve. While for the brace with  $P_e/P_y$  of 2, global buckling is fully restricted and the frame resists lateral loading successfully. Under monotonically increasing loading causing compression in the member, the buckled TiTBRB with  $P_e/P_y$  of 1.5 is shown in Fig. 17(a) while the sound TiTBRB with  $P_e/P_y$  of 2 is shown in Fig. 17(b).

From Fig. 16, it can also be seen that compressive load carrying capacity of the TiTBRBF with  $P_e/P_y$  of 2, is slightly higher than its tensile load carrying capacity, which is related to the positive effect of the frictional contact between the inner core tube and the external restraining one on increasing the compressive load-carrying capacity of the TiTBRB member.

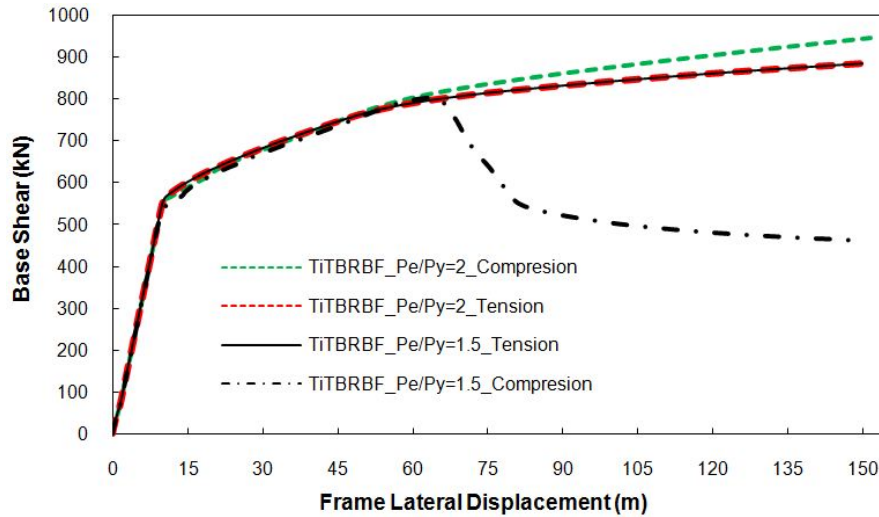
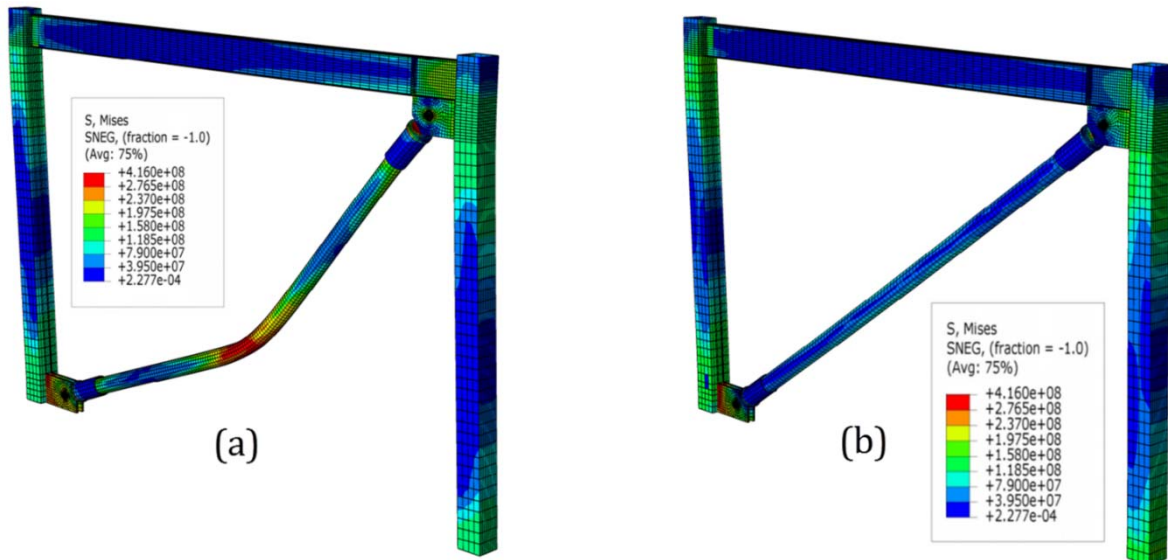


Fig. 16 Monotonic load-displacement relationship of the TiTBRBF equipped with TiTBRBs with different values of the restraining ratio ( $P_e/P_y$ )



(a) The buckled TiTBRB with restraining ratio of  $P_e/P_y = 1.5$

(b) TiTBRB with restraining ratio of  $P_e/P_y = 2$

Fig. 17 The behavior of TiTBRB in the braced frame level within monotonic loading condition

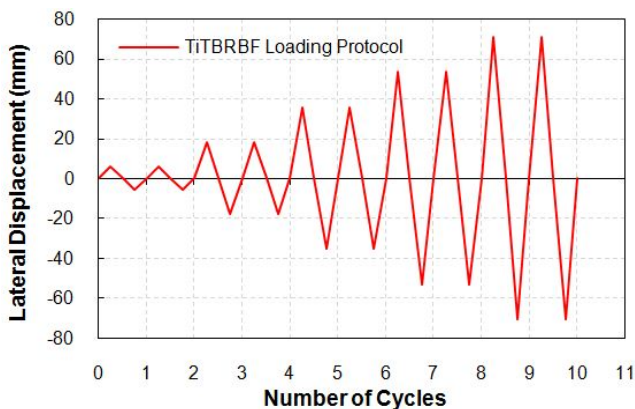


Fig. 18 Displacement protocol used for cyclic loading

#### 4.2 Cyclic analysis of the frame equipped with TiTBRB

In order to investigate the TiTBRBF behavior under reversible cyclic loading, the AISC loading protocol has been applied to the frame as lateral displacement. This protocol is calculated based on lateral story drift of %1 and is shown in Fig. 18.

As demonstrated in the previous section, the TiTBRBF with brace restraining ratio of 1.5, buckled globally under the application of monotonic loading, hence is not considered here for cyclic analysis. Accordingly, the FE model of the TiTBRBF frame with a restraining ratio of 2 has been analyzed applying the mentioned loading protocol under displacement control. The resulting hysteresis curve of the TiTBRBF is illustrated in Fig. 19.

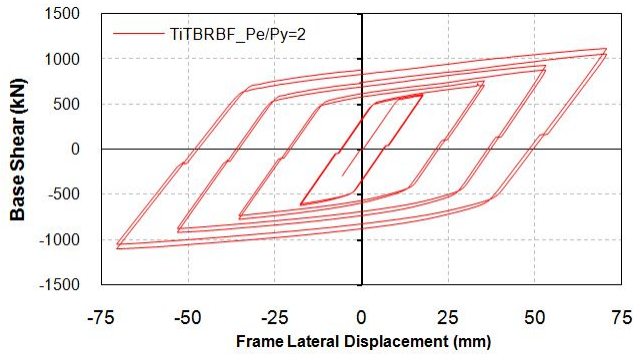


Fig. 19 Hysteresis curve of the TiTBRBF with the brace restraining ratio ( $P_e/P_y$ ) of 2

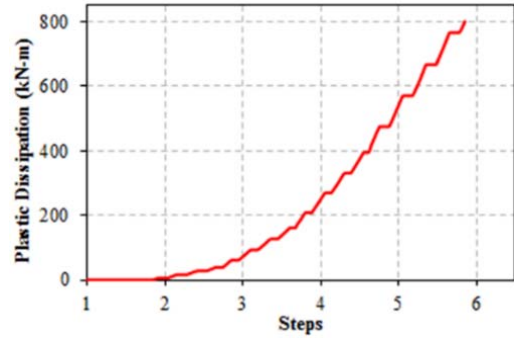


Fig. 21 Plastic energy during cyclic loading of TiTBRBF under study

The deformed shape of the inner core tube corresponding to the displacement of 2% drift is presented in Fig. 20. It should be noted that the outer tube is hidden from the model in order to make the core deflection clearly visible. In addition, the plastic energy absorbed during cyclic loading of TiTBRBF is also displayed in Fig. 21. As shown in the figure, since the loading protocol starts with 2 cycles at  $\Delta y$ , thus no plasticity occurs and the dissipated plastic energy is zero during first two steps. From step 2 onward, as the loading steps increase the amount of dissipated plastic energy upsurges gradually.

### 5. Application of the backbone curve to simplified frame modeling

In previous sections, the individual TiTBRBs have been simulated numerically and analyzed using detailed models. Based on the FEA results, the monotonic load-displacement diagram, the hysteresis curve, the backbone curve and design related parameters have been determined for individual TiTBRB members. The analyzed TiTBRBs have then been located in a single span- single story frame and the detailed finite element models of the frames equipped

with such TiTBRBs have been constructed using a combination of solid and shell elements in order to capture the behavior of the TiTBRB at the frame level as accurate as possible. It was shown in section 4 that the detailed model of the TiTBRBF incorporating solid and shell elements, was capable of demonstrating clearly the behavior of all parts of the frame during cyclic loading. In addition, stress propagation could be followed accurately. However, from a numerical modeling point of view, solving such a frame FE model which includes material and geometric nonlinearities as well as extensive contact nonlinearities is a tedious work for a multi span-multi story TiTBRBF.

Finite element modeling with the use of beam elements can be an efficient alternative to the approximate global response of a TiTBRBF only if the TiTBRB member behavior can be properly assigned to the model. In this regard, the linear and nonlinear backbones can be defined in ABAQUS using advanced connector elements provided in the software. Accordingly, in the current section, the single-bay single-story frame which was modeled using solid/shell elements in previous sections, is modeled and analyzed using beam elements in an effort to lessen the computational cost and time and to estimate the accuracy of the results of the simplified TiTBRBF model.

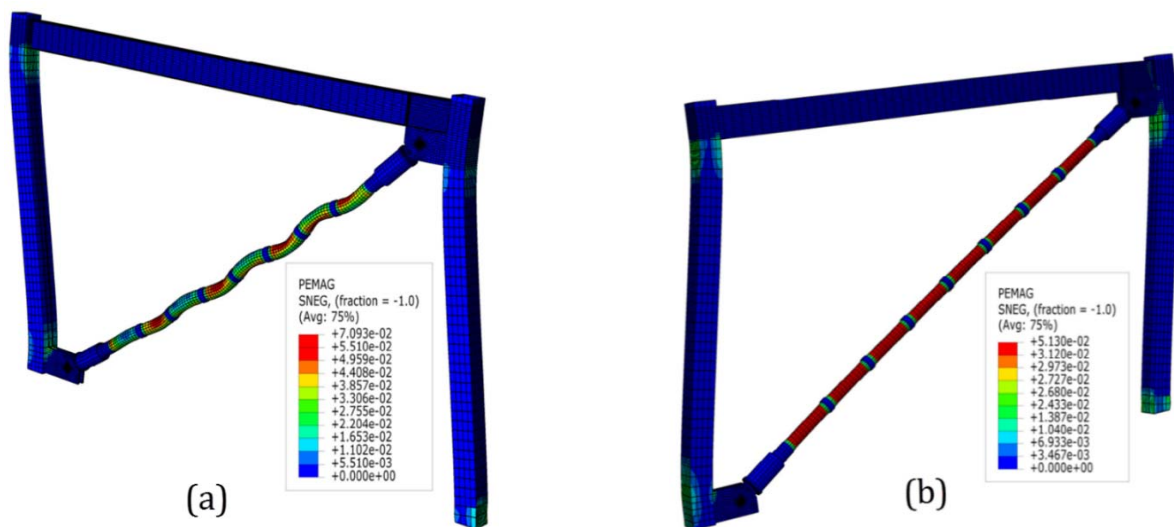


Fig. 20 The deformed shape of the inner core tube in TiTBRBF during cyclic loading: (a) The drift of 2% compressive displacement; (b) The drift of 2% tensile displacement

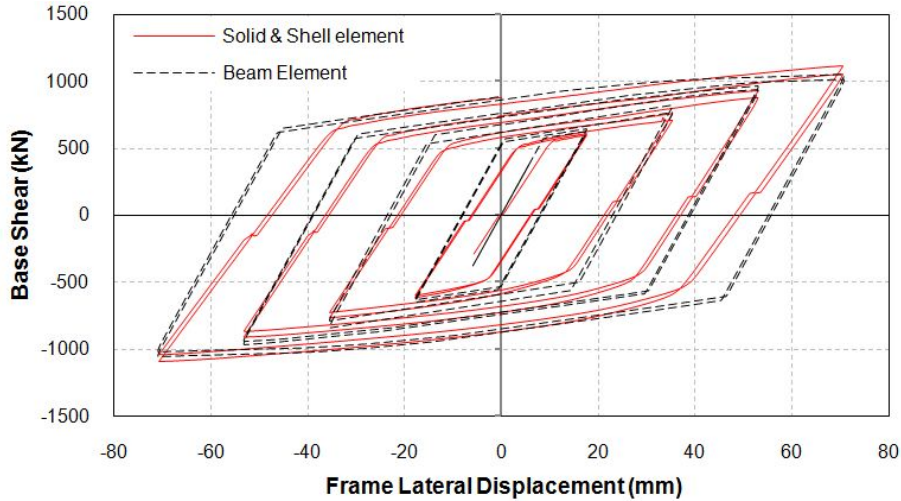


Fig. 22 Comparison between hysteresis curve of the TiTBRBF modeled using beam and solid/shell elements

Here, the beam and columns have been modeled by using the nonlinear beam elements. They have been designated as B32 in ABAQUS. The TiTBRB also, has been represented by means of connector elements in such a manner that the desired multi-linear backbone curve is assigned to the connector element to simulate its behavior. Fig. 22 shows the resulting hysteresis curve of TiTBRBF using beam element with properly defined backbone curve. For comparison, the hysteresis curve of the TiTBRBF using solid/shell elements is also shown in the figure. As shown in the figure, the hysteresis curves are in close agreement with each other.

Although beam elements result in much less run time and computational efforts, they suffer some drawbacks. In more clear words, as shown in section 3.3, both TiTBRBs with restraining ratios of 1.5 and 2 have stable hysteresis behavior resulting in identical backbone curve as far as individual BRB element behavior is concerned. However, as illustrated in section 4.1, considering the type of details

used at both ends of the TiTBRB, the TiTBRB with restraining ratio of 1.5 has no longer been capable of resisting the flexural bending exerted from the frame in the TiTBRBF system, thus in the case of this member, global buckling has taken place, while the TiTBRB with a restraining ratio of 2 has resisted monotonically increasing lateral loading with no sign of buckling. This phenomenon which is dependent upon the overall frame behavior and TiTBRB end connection details has not been observed in the frame simplified model since the equivalent brace element has been defined to represent the behavior of the individual TiTBRB member at the frame level.

These observations emphasize the necessity of detailed numerical simulations and experimental tests at both the TiTBRB element level and the TiTBRBF (frame) level as instructed by the AISC provisions for BRBs in order to approximate the actual frame behavior when equipped with such TiTBRB considering the effects of connections. In order to better approximate the full frame behavior based on

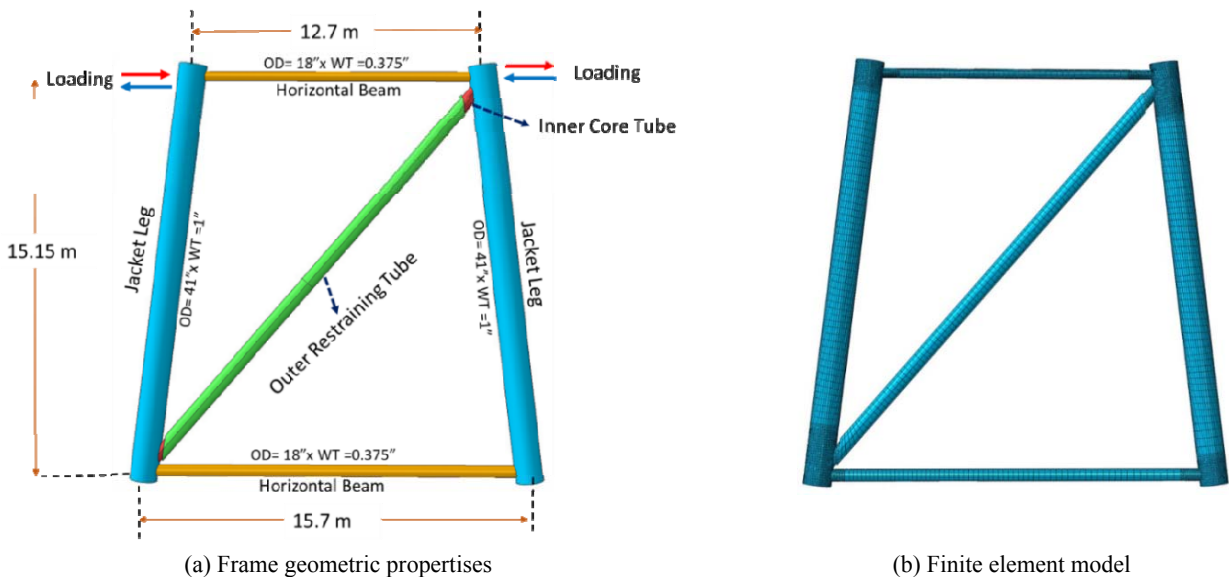


Fig. 23 Application of the introduced TiTBRB in a typical frame of offshore jacket platforms

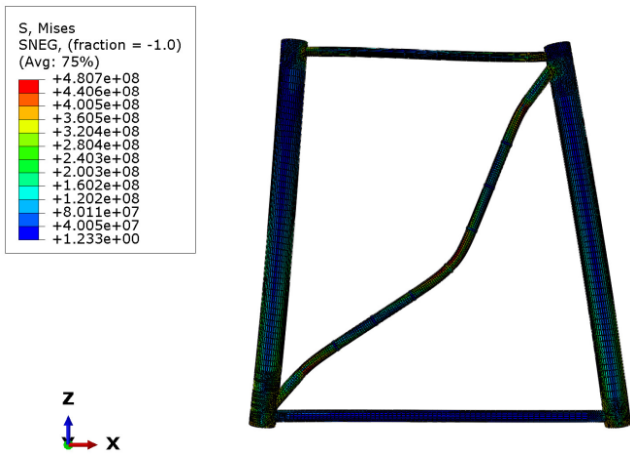


Fig. 24 Buckling of the existing non-BRB brace during cyclic loading

the individual BRB member, the connection details need be so designed to reduce the influence of the full frame on the TiTBRB member behavior.

### 6. Application of proposed TiTBRB to offshore Structures

In the previous sections, it has been shown that the proposed TiTBRB is technically competent to act as a competitive all-steel buckling restrained brace. In this section, we developed a study to investigate the cyclic performance of the proposed TiTBRB in a typical offshore jacket platform, once verified that the proposed TiTBRB complies with the AISC criteria for buckling restrained braces in both the individual BRB level and the frame level. The considered configuration for the TiTBRB matches with tubular members of structures, especially steel offshore platforms. In a typical fixed steel offshore platform, all members including legs, braces and horizontal beams are constructed using circular hollow sections. The introduced tube-in-tube BRBs also contain circular hollow sections, therefore it is expected that the TiTBRB can be easily

implemented in those offshore platforms. To accomplish this idea, a typical frame of fixed offshore platforms has been considered to be equipped with the TiTBRB. The detail of the selected frame is presented in Fig. 23(a). The cyclic performance of the selected offshore frame has been investigated under the application of cyclic loading using the same procedure described for the building frame in the previous sections. The finite element model of the offshore frame is shown in Fig. 23(b).

For the purpose of better comparison, the selected offshore frame has also been simulated and analysed with an ordinary non-BRB brace. The cross-section properties of the ordinary brace are similar to the inner core tube considered for TiTBRB. Both frames has been analysed under same loading protocol. Based on the analyses results, the ordinary non-BRB brace suffers from buckling under compressive loads as shown in Fig. 24. While, in the case of TiTBRB, buckling is successfully restricted and a stable and symmetric hysteresis behavior is achieved. The resulting hysteresis curves are shown in Fig. 25 for both models. As shown in the figure, with the aid of TiTBRB, the hysteresis behavior and load carrying capacity of the offshore frame has been improved significantly. The deformation of the inner core tube is depicted in Fig. 26. It should be mentioned that the outer retraining tube has been hidden to make the inner one visible.

### 7. Conclusions

In the present study, the concept of TiTBRB as a new kind of all-steel BRBs has been dealt with both at the individual member and the overall frame level. Through detailed FE analysis, the behavior of such individual TiTBRBs, as well as full frame composed of such TiTBRBs, have been investigated under the application of both monotonic and cyclic loading condition. It has also been demonstrated that the proposed TiTBRB can be implemented in an offshore jacket platform.

- According to the acceptance criteria prescribed by the AISC 34-10 for BRBs, and based on the detailed FEA results, it has been demonstrated clearly that the

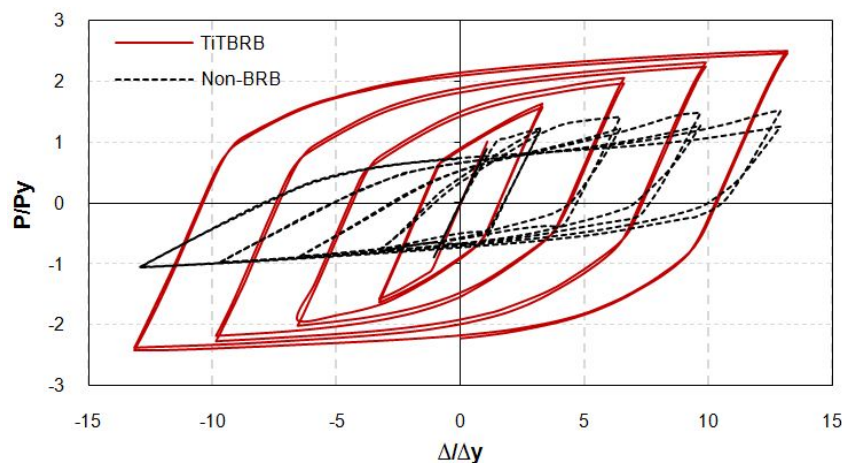


Fig. 25 Hysteresis curves of the offshore frames with and without TiTBRB

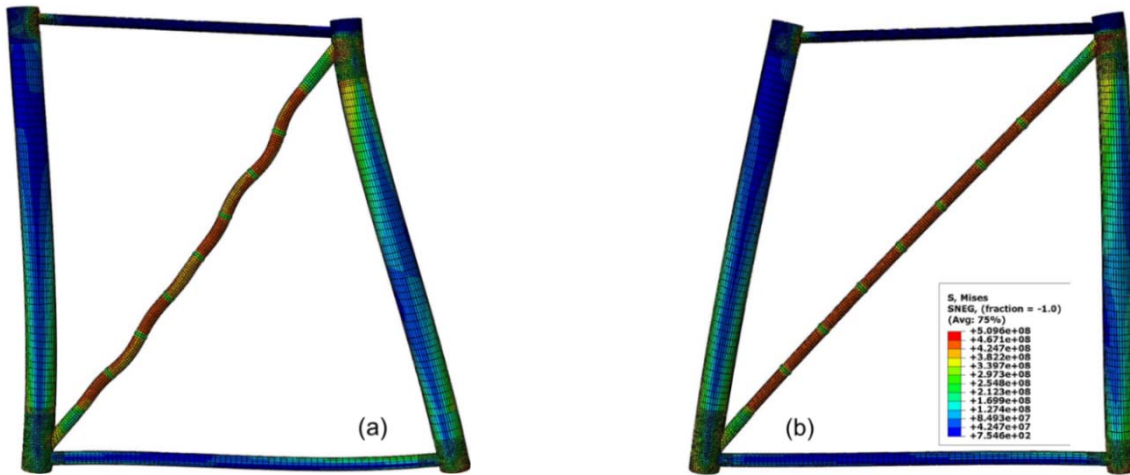


Fig. 26 The inner core tube deformation at drift of 2%: (a) compressive deformation; (b) tensile deformation

proposed TiTBRB member is technically competent to act as an all-steel buckling restrained brace. Therefore, the proposed TiTBRB deserves further studies through experimental investigations

- In such all-steel TiTBRBs, not only the unbonding agents are eliminated, concrete works have also been excluded from fabrication and construction work. Hence, much lighter BRB members are obtained. This is also associated with ease and speed of fabrication, erection, inspection, replacement and therefore a more economical and environmentally friendly design.
- With the use of backbone curves derived from the FE analyses, the simplified equivalent beam model has been introduced and verified through comparison with detailed FE model. Close agreement was observed between the FE results and the results of the simplified equivalent frame model. On the basis of the finite element analyses results, it was shown that in case that TiTBRB element behavior can be assigned to the brace member properly, a simplified model is capable of predicting the cyclic behavior of TiTBRB frame with sufficient accuracy for design purposes.
- The TiTBRB member which behaved satisfactorily at the brace element level within the cyclic loading condition may suffer global buckling due to possible flexural demand exerted from frame to the brace member depending upon the type of end connection details and the manner in which the TiTBRB member is connected to the beam to column connection. It should be noted that some BRB connection types, such as “spliced beam” may reduce the extra demands on the connection region.
- Although the use of equivalent beam elements results in much less run time and computational efforts, they may exhibit some limitations. In more clear words, both TiTBRBs with restraining ratios of 1.5 and 2 exhibits stable hysteresis behavior resulting in identical backbone curve as far as individual BRB element behavior is concerned. However, considering the type of connections

employed in the finite element frame model, the TiTBRB with restraining ratio of 1.5 has no longer been capable of resisting the flexural bending exerted from the frame in the TiTBRBF system, hence in the case of the frame composed of this member, global buckling has taken place, while the TiTBRB with a restraining ratio of 2 has resisted lateral loading satisfactorily. This phenomenon could not be captured using the equivalent beam elements which are defined on the basis of the backbone curves which have been similar in both cases.

- These observations emphasize the necessity of detailed numerical simulations and experimental tests at both the TiTBRB element level and the TiTBRBF (frame) level as instructed by the AISC seismic provisions for BRBs. In order to achieve as close as possible the individual member behavior in a full frame model the end details play a crucial role in reducing the full frame effects on the behavior of the TiTBRB within the frame.
- The proposed TiTBRB is well suited to tubular members of offshore structures such as offshore jacket platforms and offshore wind turbines. Using detailed FE analysis, it has been shown that the TiTBRB can be utilized in offshore structures to improve their hysteresis behavior. The application of such TiTBRBs to offshore jacket platforms under seismic excitation is under study by the authors and the results will be revealed in a forthcoming paper.

## References

- AISC 341-10 (2010), Seismic provisions for structural steel buildings; *Am. Inst. Steel Constr.*, Chicago, IL, USA (1).
- AISC 360-10 (2010), Specification for Structural Steel Buildings (ANSI/AISC 360-10); *Am. Inst. Steel Constr.*, Chicago, IL, USA.
- Chou, C.C. and Chen, S.Y. (2010), “Subassemblage tests and finite element analyses of sandwiched buckling-restrained braces”, *Eng. Struct.*, **32**(8), 2108-2121.  
DOI: <http://dx.doi.org/10.1016/j.engstruct.2010.03.014>
- Clough, R.W. and Penzien, J. (1993), *Dynamics of Structures*, (2nd

- ed.), McGraw-Hill.
- Della Corte, G., D'Aniello, M. and Landolfo, R. (2014), "Field testing of all-steel buckling-restrained braces applied to a damaged reinforced concrete building", *J. Struct. Eng.*, **141**(1), D4014004.
- Dongbin, Z., Xin, N., Peng, P., Mengzi, W., Kailai, D. and Yabin, C. (2016), "Experimental study and finite element analysis of a buckling-restrained brace consisting of three steel tubes with slotted holes in the middle tube", *J. Constr. Steel Res.*, **124**, 1-11.
- Fahnestock, L.A., Sause, R. and Ricles, J.M. (2003), "Analytical and experimental studies on buckling restrained braced composite frames", In: *Proceedings of the International Workshop on Steel and Concrete Composite Construction (IWSCCC-2003)*, pp. 177-188.
- Fahnestock, L.A., Ricles, J.M. and Sause, R. (2007a), "Experimental evaluation of a large-scale buckling-restrained braced frame", *J. Struct. Eng.*, **133**(9), 1205-1214.
- Fahnestock, L.A., Sause, R. and Ricles, J.M. (2007b), "Seismic Response and Performance of Buckling-Restrained Braced Frames", *J. Struct. Eng.*, **133**(9), 1195-1204.
- Fotoohabadi, A. (2015), "An investigation of the behavior of steel frames equipped with double-tube buckling restrained braces", M.Sc. Dissertation; (Under Supervision of Shahrokh Maalek), School of Civil Engineering, College of Engineering, University of Tehran, Iran.
- Ghasemi, S. (2006), "The Introduction of a Buckling Restrained Bracing System for Steel Structures", M.Sc. Dissertation; (Under Supervision of Shahrokh Maalek), School of Civil Engineering, College of Engineering, University of Tehran, Iran.
- Heidary-Torkamani, H. and Maalek, S. (2017), "Conceptual numerical investigation of all-steel Tube-in-Tube buckling restrained braces", *J. Constr. Steel Res.*, **139**, 220-235.
- Hoveidae, N., Tremblay, R., Rafezy, B. and Davaran, A. (2015), "Numerical investigation of seismic behavior of short-core all-steel buckling restrained braces", **114**, 89-99.  
DOI: <http://dx.doi.org/10.1016/j.jcsr.2015.06.005>
- Jia, L.J. and Kuwamura, H. (2014), "Prediction of cyclic behaviors of mild steel at large plastic strain using coupon test results", *J. Struct. Eng.*, **140**(2), 04013056.  
DOI: <http://ascelibrary.org/doi/10.1061/%28ASCE%29ST.1943-541X.0000848> (October 15, 2016).
- Jiang, Z., Guo, Y., Zhang, B. and Zhang, X. (2015), "Influence of design parameters of buckling-restrained brace on its performance", *J. Constr. Steel Res.*, **105**, 139-150.  
DOI: <http://dx.doi.org/10.1016/j.jcsr.2014.10.024>
- Kersting, R.A., Fahnestock, L.A. and Lopez, W.A. (2015), "Seismic design of steel buckling-restrained braced frames - a guide for practicing engineers", NEHRP Seismic Design Technical Brief No. 11, (11).
- Korzekwa, A. and Tremblay, R. (2009), "Numerical simulation of the cyclic inelastic behaviour of buckling restrained braces", In: *Behaviour of Steel Structures in Seismic Areas*, CRC Press.  
DOI: <http://dx.doi.org/10.1201/9780203861592.ch94>
- Lopez, W.A., Gwie, D.S., Lauck, T.W. and Saunders, C., (2004), "Structural design and experimental verification of a buckling-restrained braced frame system", *Eng. Journal, AISC*, **41**(4), 177-186.
- Maalek, S. (1999), "Structural Assessment and Quality Control Procedures for the Homa Aircraft Hangar No. 3", *Int. J. Sp. Struct.*, **14**(3), 167-184.
- Maalek, S. and Ghasemi, S. (2010), "The Introduction of a Buckling Restrained Bracing System", *Proceedings of the 14th European Conference on Earthquake and Engineering*.
- Mazzolani, F.M., James, M.R. and Richard, S. (2009), *STESSA 2009: Proceedings of the Sixth International Conference on Behaviour of Steel Structures in Seismic Areas*, Philadelphia, PA, USA, August, CRC Press.
- Merritt, S., Uang, C.M. and Benzoni, G. (2003), "Subassemblage testing of STAR SEISMIC buckling-restrained braces", Rep. No. TR-2003, 4.
- Omidi, H. (2014), "Presentation and development of the proposed double-tube system as Buckling Restrained Brace", M.Sc. Dissertation; Under Supervision of Shahrokh Maalek", School of Civil Engineering, College of Engineering, University of Tehran, Iran.
- Piedrafita, D., Maimi, P. and Cahis, X. (2015), "A constitutive model for a novel modular all-steel buckling restrained brace", *Eng. Struct.*, **100**, 326-331.  
DOI: <http://dx.doi.org/10.1016/j.engstruct.2015.06.026>
- Sabelli, R., Mahin, S. and Chang, C. (2003), "Seismic demands on steel braced frame buildings with buckling-restrained braces", *Eng. Struct.*, **25**(5), 655-666.  
DOI: <http://www.sciencedirect.com/science/article/pii/S014102960200175X> (August 1, 2015)
- SIMULIA (2007), ABAQUS analysis and theory manual; Karlsson, and Sorensen Inc, Providence, RI, USA.
- Takeda, Y., Kimura, Y., Yoshioka, K., Furuya, N. and Takemoto, Y. (1976), "An Experimental Study on Braces encased in Steel Tube and mortar", In: *Annual Meeting Architectural Institute of Japan*, pp. 1041-1042.
- Tremblay, R., Bolduc, P., Neville, R. and DeVall, R. (2006), "Seismic testing and performance of buckling-restrained bracing systems", *Can. J. Civil Eng.*, **33**(2), 183-198.  
DOI: <http://www.nrcresearchpress.com/doi/abs/10.1139/105-103> (October 11, 2016)
- Watanabe, A., Hitomi, Y., Saeki, E., Wada, A. and Fujimoto, M. (1988), "Properties of brace encased in buckling-restraining concrete and steel tube", In: *Proceedings of Ninth World Conference on Earthquake Engineering*, 719-724.
- Yin, Z. and Bu, F. (2016), "Overall Stability Analysis of Improved Buckling Restrained Braces", *Open Civ. Eng. J.*, **10**(1), 61-75.
- Yin, Z.Z. and Wang, X.L. (2010), "Hysteretic Performance Analysis of Double-Tube Buckling Restrained Braces with Contact-Ring", *Adv. Mater. Res.*, **163-167**, 681-685.
- Yin, Z.Z., Wang, X.L. and Li, X.D. (2011), "An Experimental Study on Double-Tube Buckling Restrained Braces with Contact Rings", *Adv. Mater. Res.*, **163-167**, 475-480.

BU